Nickel Catalyst Based on Three-dimensional Carbon Nanotube Sponge as Free-standing Electrode for Efficient Water Electrolysis

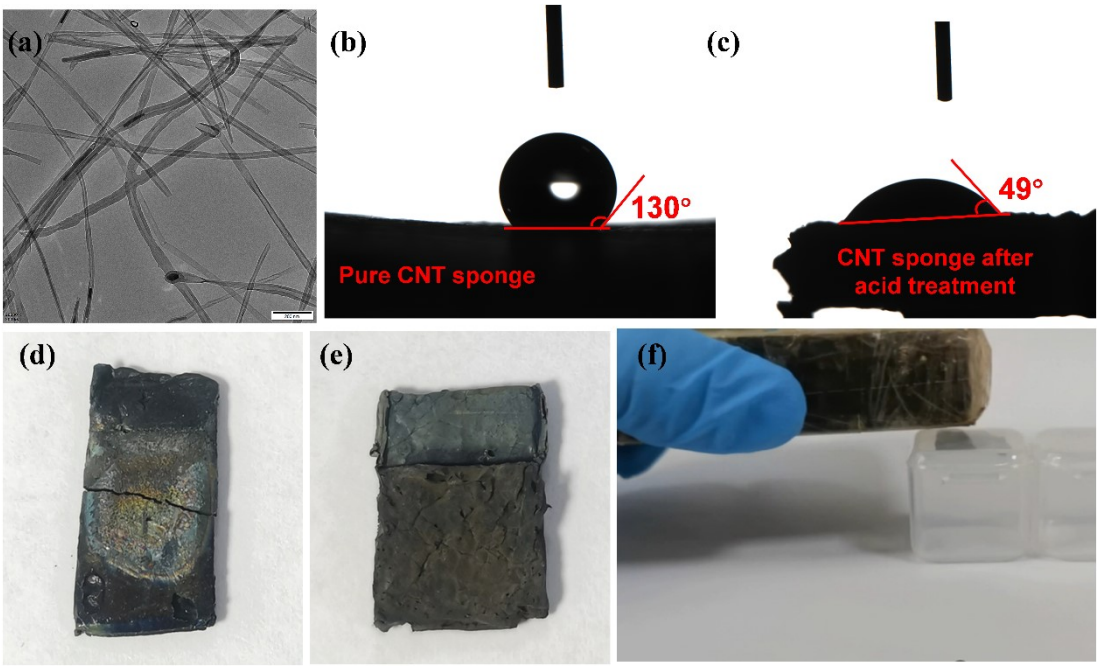

Figure S1. Hydrophilicity test of CNT before and after acid treatment and optical photographs after electroplating. (a) TEM image of a carbon nanotube sponge (b) Hydrophilicity test prior to acid treatment; (c) Hydrophilicity test after acid treatment; (d) Optical photographs of acid-free electroplating; (e) Optical photographs of acid treatment after plating. (f)

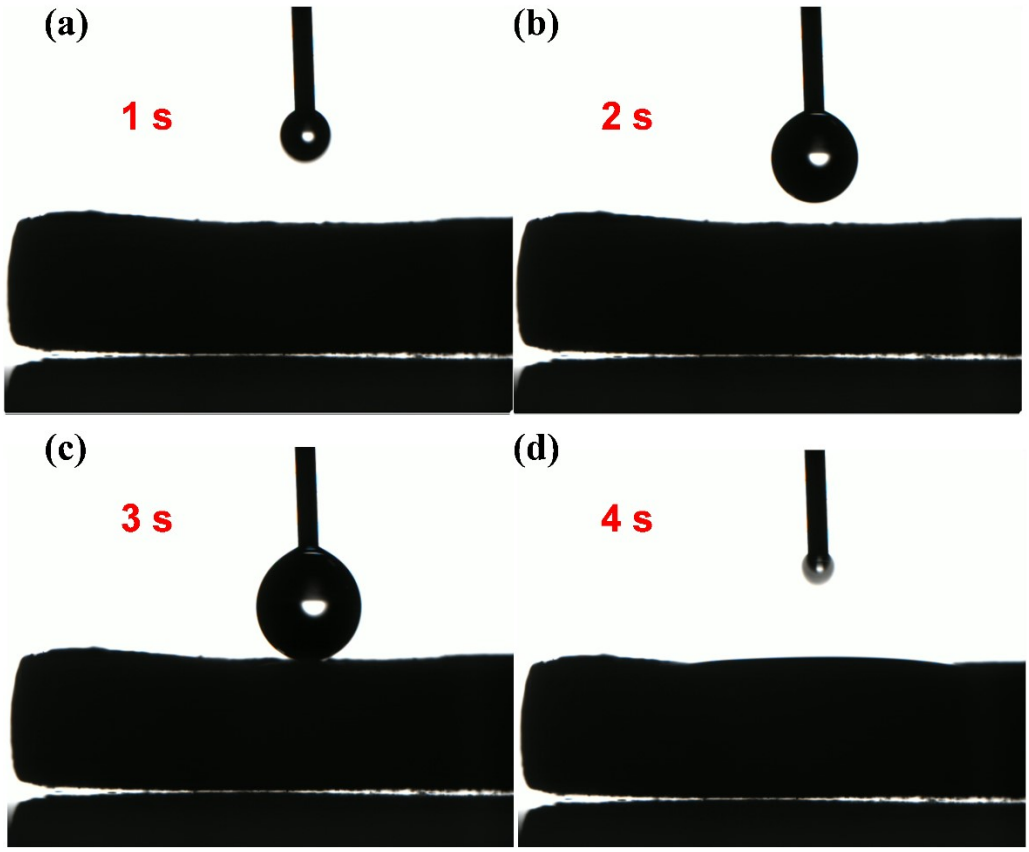

Figure S2. Hydrophilicity test of Ni/CNT. (a)1s; (b)2s; (c) 3s and (d) 4s.

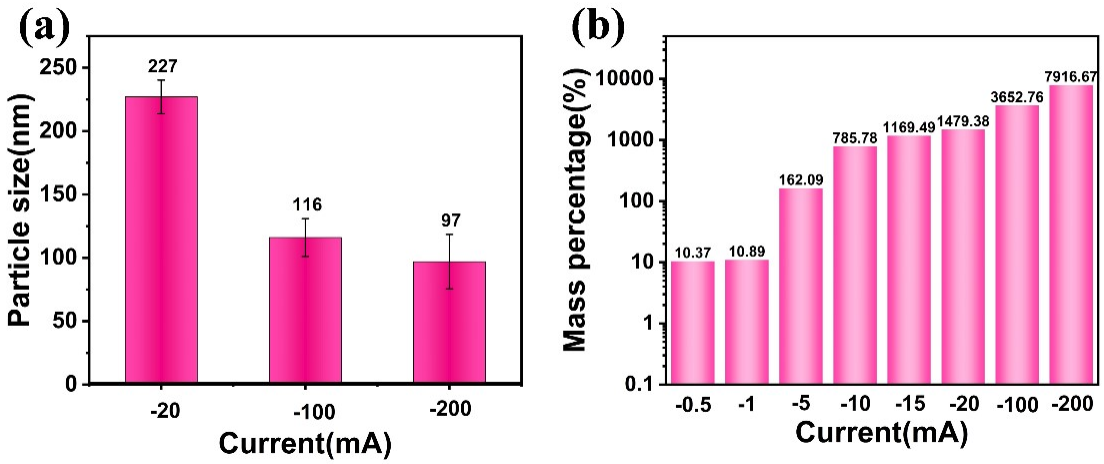

Figure S3. (a) Statistical diagram of particle size under different currents; (b) Statistical diagram of the mass increase of the sponge after electroplating under different currents.

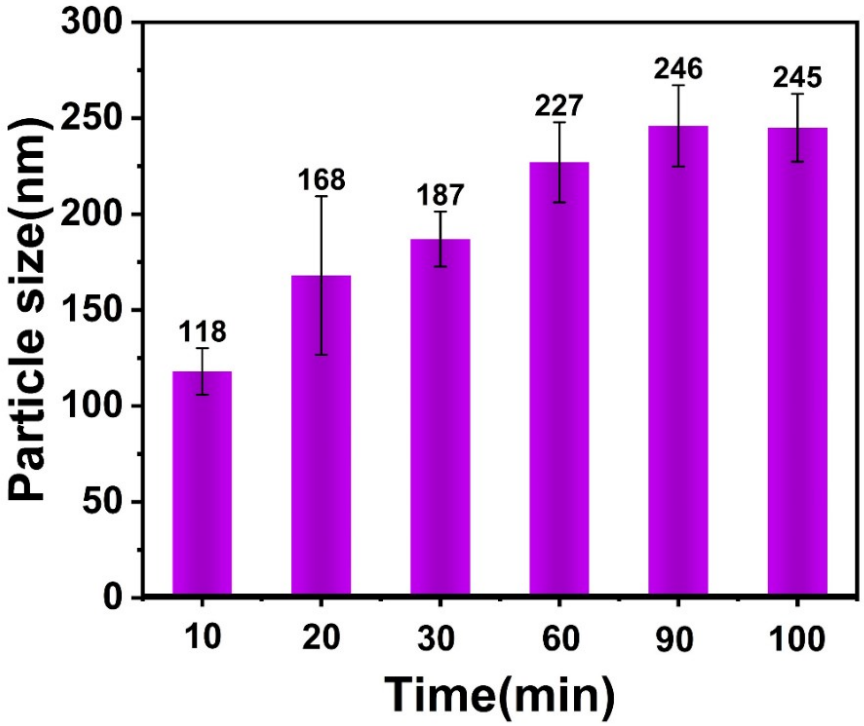

Figure S4. Particle size statistics of different times of plating at the same plating current

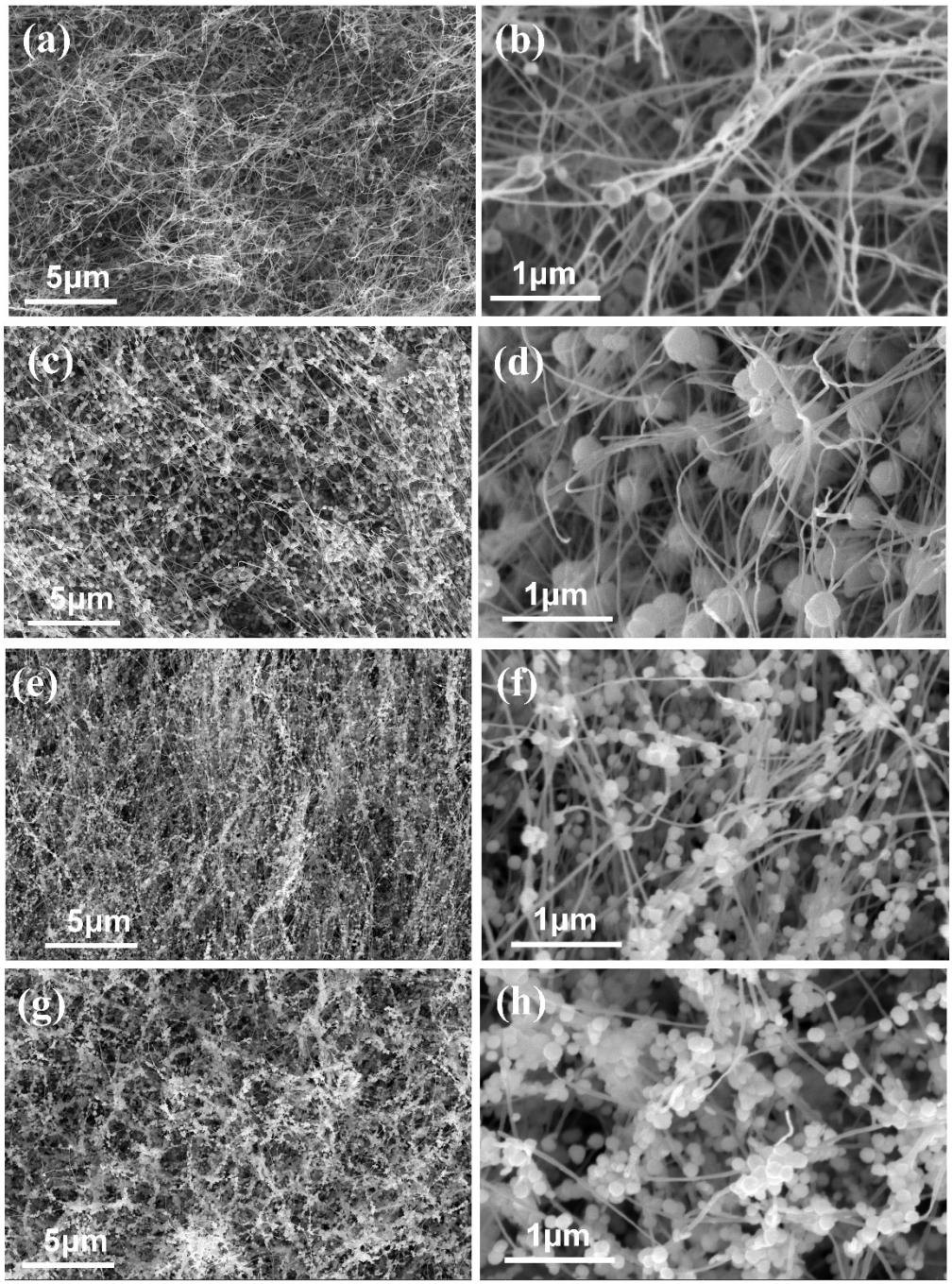

Figure S5. SEM images of composite electrodes were prepared at the same time and at different currents for plating at the same time. (a, b) SEM images at different magnifications at -10 mA; (c, d) SEM images at different magnifications at -20 mA; (e, f) SEM images at different magnifications at -100 mA; (g, h) SEM images at different magnifications at a current of -200 mA.

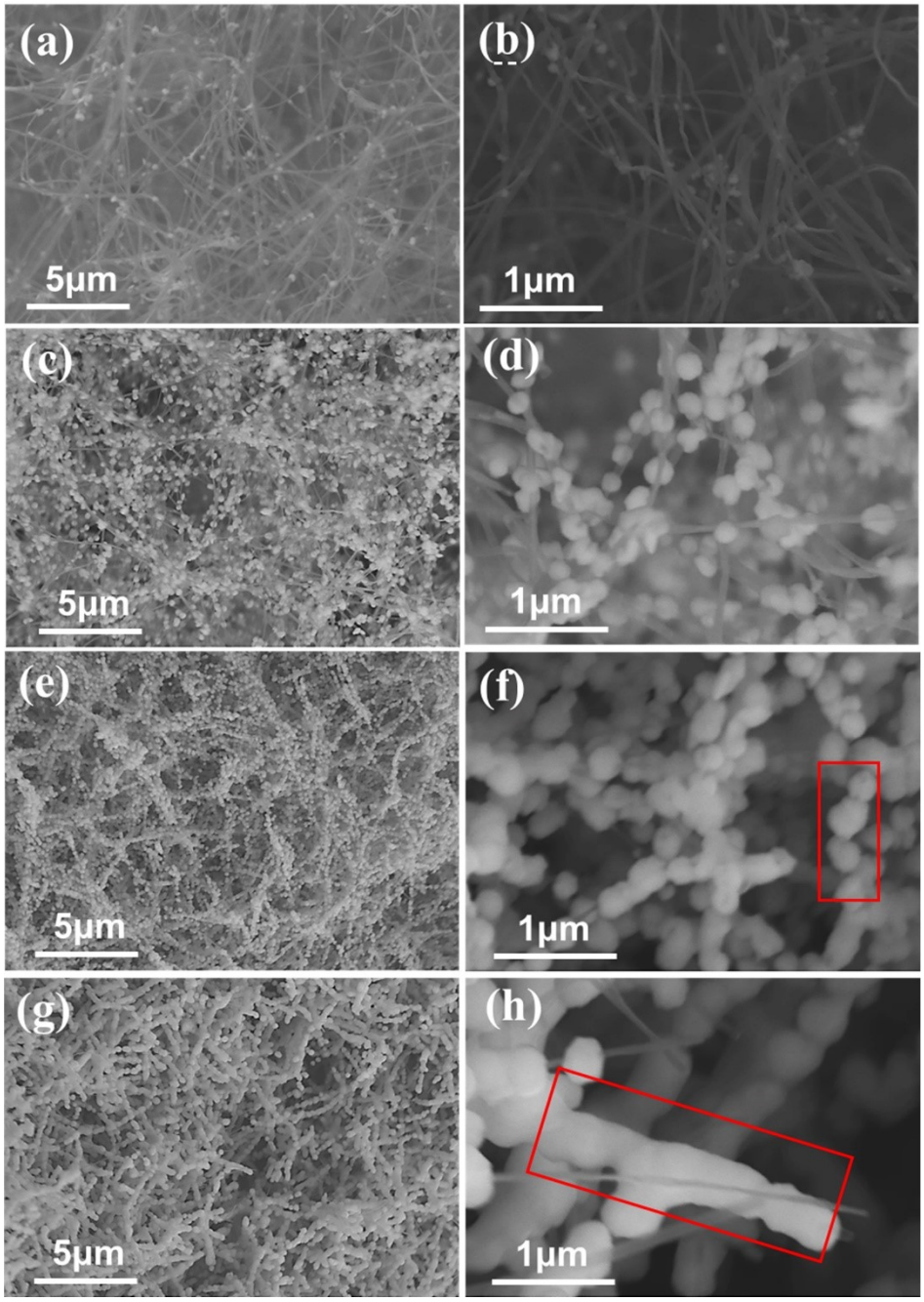

Figure S6. SEM image of a composite electrode with the same plating current and different plating times. (a, b) SEM images of different multiples after 10 min of plating at -20 mA; (c, d) SEM images of different multiples after 30 min of plating at -20 mA; (e, f) SEM images of different multiples after 60 min of plating at -20 mA; (g, h) SEM images of different multiples after plating for 90 min at a plating current of -20 mA.

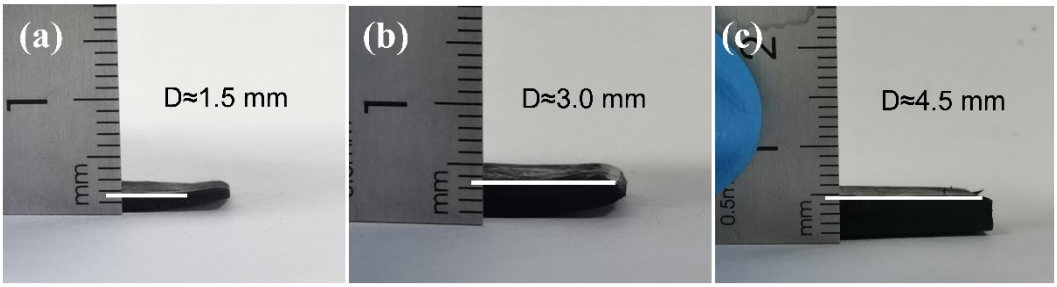

Figure S7. Physical drawings of CNT sponges of different thicknesses. (a) The thickness of the CNT sponge was 1.5 mm after 0.5 h of growth; (b) The thickness of the CNT sponge was 3.0 mm after 1.5 h of growth; (c) The thickness of the CNT sponge was 4.5 mm after 2.5 h of growth.

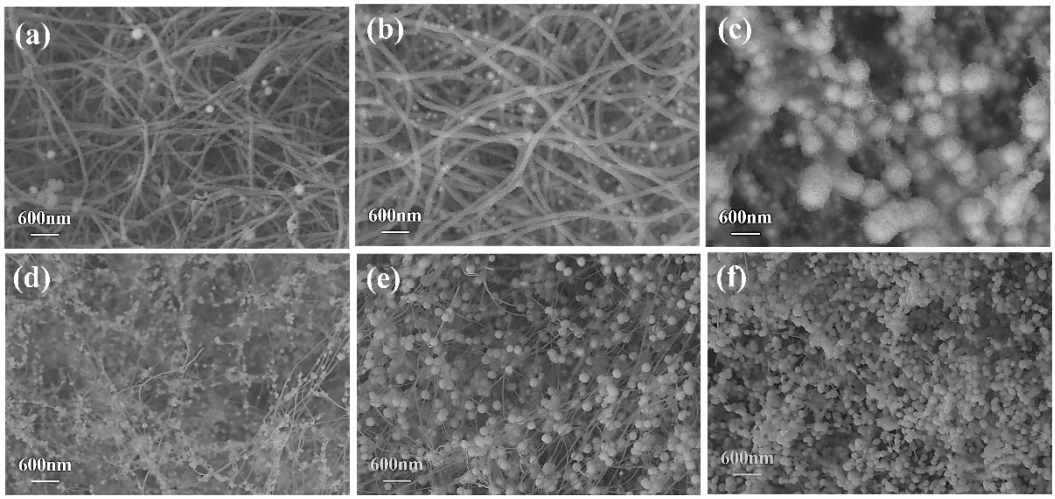

Figure S8. SEM images of the surface and interior of the sponge after plating with different sponge thicknesses at the same plating current and time. (a) and (d) surface and internal morphology of CNT sponge with a thickness of 0.5 mm; (b) and (e) surface and internal morphology of CNT sponge with a thickness of 3.0 mm; (c) and (f) Surface and internal morphology of CNT sponge with a thickness of 4.5 mm.

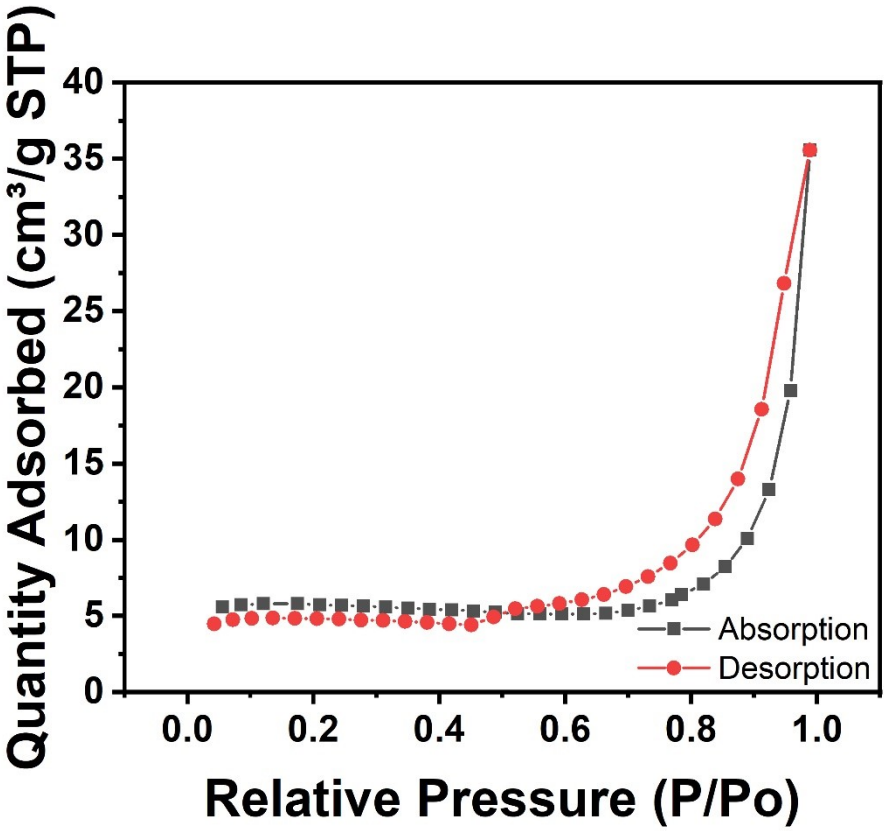

Figure S9. Nitrogen adsorption and desorption curves of Ni/CNT-60 composites

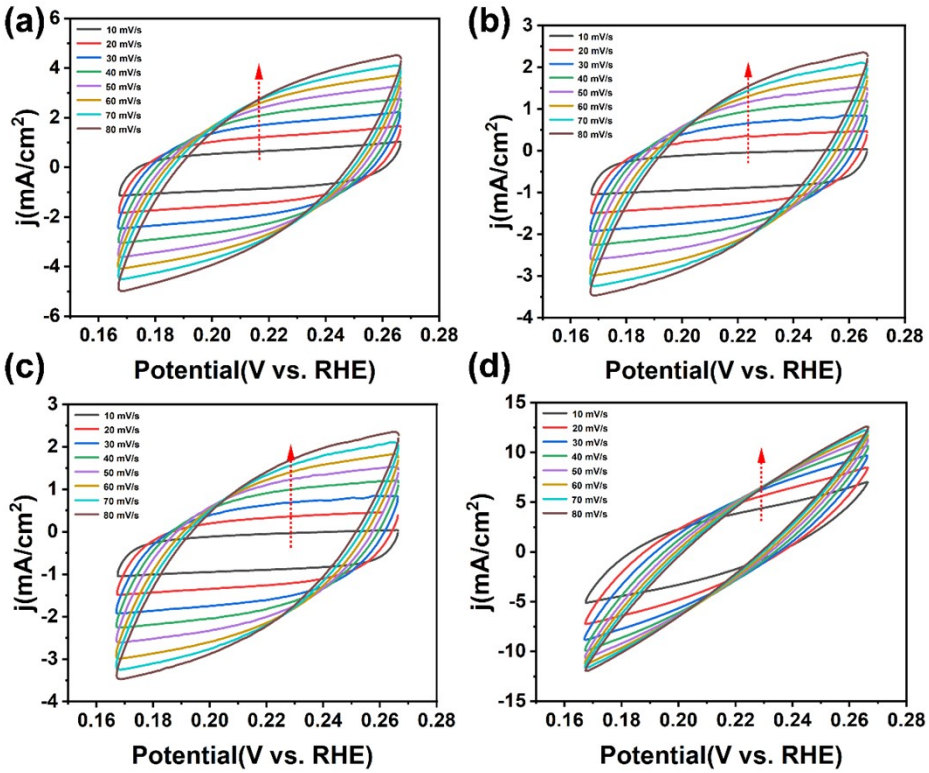

Figure S10. CV plots of HER at different sweep speeds. (a) CV diagram of Ni/CNT-10 at different sweep speeds; (b) CV diagram of Ni/CNT-30 at different sweep speeds; (c) CV diagram of Ni/CNT-60 at different sweep speeds; (d) CV diagram of Ni/CNT-90 at different sweep speeds.

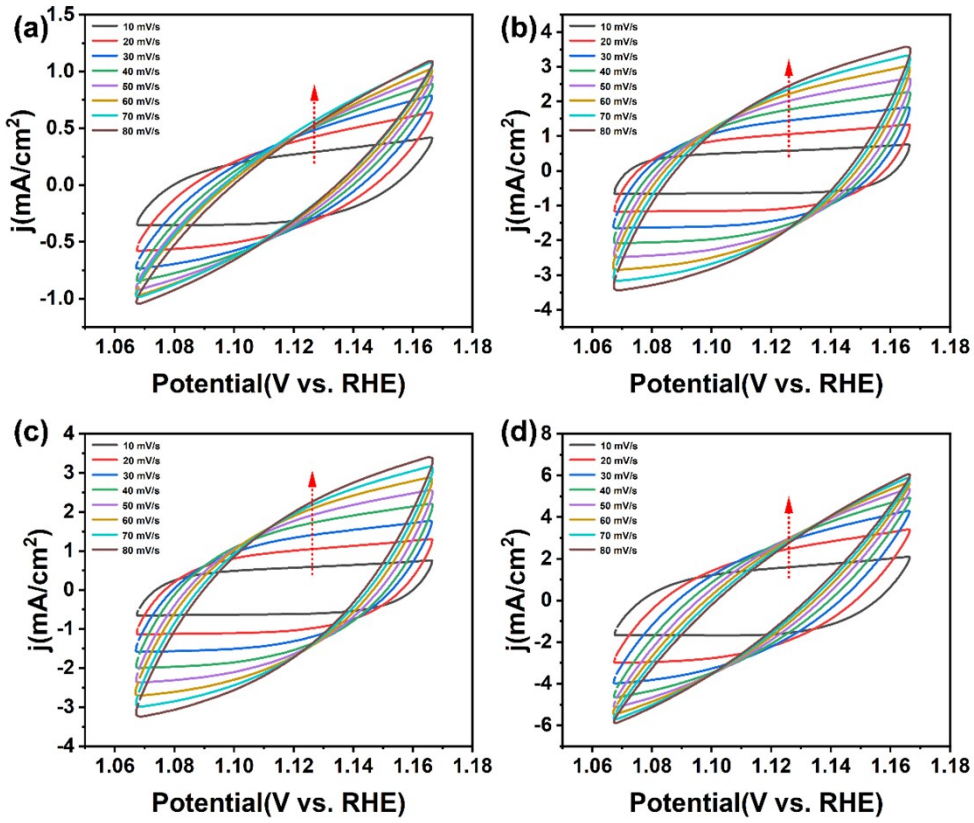

Figure S11. CV plot of OER at different sweep speeds. (a) CV diagram of Ni/CNT-10 at different sweep speeds; (b) CV diagram of Ni/CNT-30 at different sweep speeds; (c) CV diagram of Ni/CNT-60 at different sweep speeds; (d) CV diagram of Ni/CNT-90 at different sweep speeds.

Table S1. The ICP of Ni/CNT catalysts.

	Wt. %	At. %
Ni	99.17%	96.08%
Others (C et al.)	0.83%	3.92%

Table S2. Comparison of HER performances for Ni/CNT-60 in 1 M KOH with that of reported catalysts.

Catalyst	Overpotential at 10 mA cm^{-2} (mV)	Tafel slope (mV dec^{-1})	Reference
Ni/CNT-60	79	37	This work
Ni-N/CMF	76.9	167	*Chem. Eng. J. 2024, 484, 149406*
CoNiP/NF	147	51	*Appl. Surf. Sci. 2021, 569, 150762*
B-Ni_2P/NF	45	128.29	*J. Alloys Compd. 2024, 984, 173974*
NiCoCu-$Mo_{0.078}$/CF	35	50.13	*Adv. Funct. Mater. 2024, 34, 2404055*
Ni−Mo nanopowder	80	20	*ACS Catal. 2013, 3, 166–169*
$CoNi_4$	53	68.08	*J. Alloys Compd. 2019, 791, 779e785*
Co_2Ni alloy/N-CNTs	100	87	
SFCA-NiCo	179	40	*Int. J. Hydrogen Energy 2021, 46 21525*
CoNi−OOH-30(40)	210	67	*Electrochim. Acta 2019, 301 449e457*
CoNi-LDH@CoNi	69	89	*Int. J. Hydrogen Energy 2021, 46 22789*
NiCo-300	156	82.7	*J. Alloys Compd. 2019, 797, 1216e1223*
$MNi_{63}Co_{37}/rGO_5$	115	45	*J. Colloid Interface Sci. 2021, 599 603–610*
hCT-$Co_{0.4}Ni_{0.6}$	150	126	*Sustainable Energy Fuels,2020, 4,369–379*
NiCo–CeO_2/GP	34	49.1	*Adv. Sustainable Syst. 2020, 4, 2000122*
NiCo (S-30)	107	119	*Appl. Surf. Sci. 2019, 465 846–862*
NiCo/NiCoOx	155	35	*ACS Appl. Mater.*

			Interfaces 2016, 8, 3208−3214
MD-Co/NiS_2	117	65.4	*Surf. Interfaces 2024, 46 103987*
$CoPB_2$@NiFe-OH/NF	32	81.6	*Green. Energy. Environ. 2024*
CoNi-N/CMF	36.6	102	*Chem. Eng. J. 2024, 484, 149406*
$NiCoRu_{0.2}$/SP	59	53	*Appl. Catal., B 2023, 331, 122710*
$Ni(OH)_2$/NiO-C/WO_3	53	92	*Chem. Eng. J. 2022, 433, 134497*

Table S3. Comparison of OER performances for Ni/CNT-60 in 1 M KOH with that of reported catalysts.

Catalyst	Overpotential at 10 mA cm^{-2} (mV)	Tafel slope (mV dec^{-1})	Reference
Ni/CNT-60	180	49	**This work**
LNFO	396	58.8	*Appl. Catal., B 2023, 330 122661*
Co-Ni-Fe-LDH	314	37.63	*J. Colloid Interface Sci. 2025, 678, 924–933*
CoNiP/NF	234	47	*Appl. Surf. Sci. 2021, 569 150762*
FeNi–rGO LDH	195	39	*Angew. Chem. Int. Ed. 2014, 53,7584 –7588*
$(Ni,Co)Se_{0.85}$	255	79	*Adv. Mater. 2016, 28, 77–85*
$NiSe_2$-DO	241	32	*Nat Commun 2016, 7, 12324*
Ni_3N nanosheets	350	85	*J. Am. Chem. Soc. 2015, 137, 4119−4125*
Ni_2P	290	59	*Energy Environ. Sci., 2015, 8,2347*
$Fe_5Co_5Ni_5O_yHz$@NFF	181	32.1	*Carbon Energy,2025*
NiCo-400	340	72.8	*J. Alloys Compd. 2019, 797 1216e1223*
$NiCo(OH)_2$–CeO_2	175	28.4	*Adv. Sustainable Syst. 2020, 4, 2000122*
$NixCo_3$−xO_4	337	75	*ACS Appl. Mater. Interfaces 2016, 8, 3208−3214*
Au-CoNiSx/NF	305.9	60.98	*ACS Appl. Nano Mater. 2024, 7, 9062−9067*
Fe_2WO_6@Ni_3S_2-WS_2/NF	170	48.26	*Sustain. Mater. Techno. 202543 e01302*
MoO_x/Ni_3S_2/NF	136	50	*Adv. Funct. Mater. 2016, 26, 4839–4847*
$Ni/Ni(OH)_2$	270	70	*Adv. Mater. 2020, 32, 1906915*
N-$NiMoO_4$/Ni/CNTs	330	89.5	*Small 2023, 19, 2207196*
NieCoeCeO_2/Ni	324	43.78	*Int. J. Hydrogen Energy 2023 48 4287-4299*
Ni/NiO/C	286.4	54.8	*New J. Chem., 2024, 48, 10133–*

			10141
NiFe@NiFe	241	60.06	*Small 2024, 20,2400046*
Ni/NiO-C	370	114	*New J. Chem., 2024, 48, 10133–10141*

Table S4. The ECSA of Ni/CNT catalysts under different plating times in 1 M KOH in HER.

Catalyst	C_{dl} (mF cm^{-2})	C_{DL} (mF)	ECSA (cm^2)
Ni/CNT-10	0.94	0.94	23.5
Ni/CNT-30	11.75	11.75	293.75
Ni/CNT-60	59.93	59.93	1498.25
Ni/CNT-90	4.58	4.58	114.5

*** $C_{DL} = C_{dl} \times 1\ cm^2$; ECSA = C_{DL}/C_s, $C_s = 0.04$ mF cm^{-2}.**

Table S5. The ECSA of Ni/CNT catalysts under different plating times in 1 M KOH in OER.

Catalyst	C_{dl} (mF cm^{-2})	C_{DL} (mF)	ECSA (cm^2)
Ni/CNT-10	0.98	0.98	24.5
Ni/CNT-30	34.91	34.91	872.75
Ni/CNT-60	43.51	43.51	1087.75
Ni/CNT-90	7.50	7.50	187.5

*** $C_{DL} = C_{dl} \times 1\ cm^2$; ECSA = C_{DL}/C_s, $C_s = 0.04$ mF cm^{-2}.**

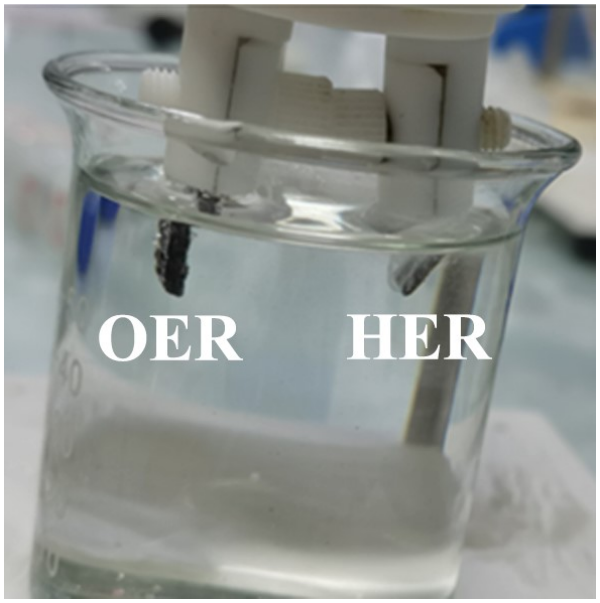

Figure S12. The device of overall water splitting.

Table S6. Conductivity of carbon nanotube sponge before and after acid treatment

	Thickness (mm)	σ (S/cm)
Before acid treatment	0.22	9.43
After acid treatment	0.20	16.53

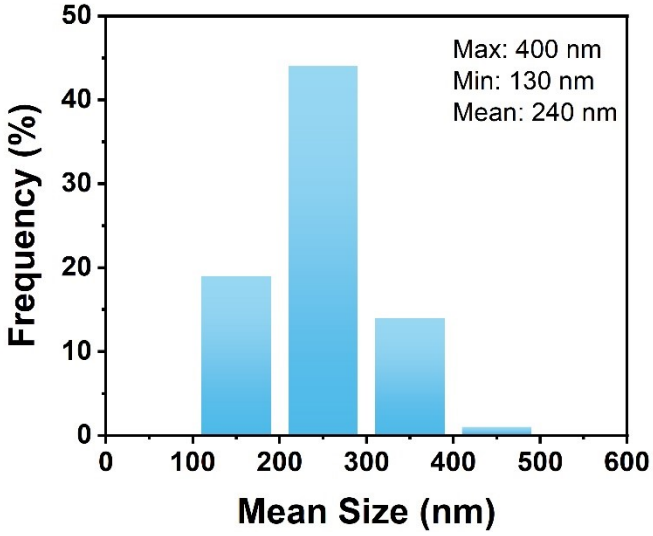

Figure S13. the particle size and distribution of Ni nanoparticles in Ni/CNT-60

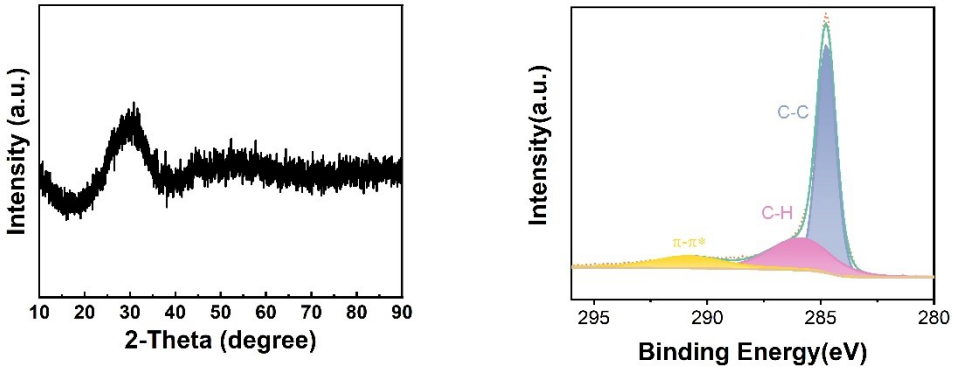

Figure S14 XRD and XPS images of carbon nanotube sponge

Figure S15 Electrochemical deposition device